Chaos, Solitons and Fractals 112 (2018) 36–43

Contents lists available at ScienceDirect

Chaos, Solitons and Fractals

Nonlinear Science, and Nonequilibrium and Complex Phenomena

journal homepage: www.elsevier.com/locate/chaos

# Computation of the largest positive Lyapunov exponent using rounding mode and recursive least square algorithm

Márcia L.C. Peixoto, Erivelton G. Nepomuceno*, Samir A.M. Martins, Márcio J. Lacerda

*Control and Modelling Group (GCOM), Department of Electrical Engineering, Federal University of São João del-Rei, Praça Frei Orlando, 170 - Centro São João del-Rei, MG, 36307-352, Brazil*

ARTICLE INFO

*Article history:*
Received 17 January 2018
Revised 19 March 2018
Accepted 23 April 2018
Available online 30 April 2018

*Keywords:*
Dynamical systems
Lyapunov exponent
Rounding mode
Lower bound error
Chaos
Recursive least square algorithm

ABSTRACT

It has been shown that natural interval extensions (NIE) can be used to calculate the largest positive Lyapunov exponent (LLE). However, the elaboration of NIE are not always possible for some dynamical systems, such as those modelled by simple equations or by Simulink-type blocks. In this paper, we use rounding mode of floating-point numbers to compute the LLE. We have exhibited how to produce two pseudo-orbits by means of different rounding modes; these pseudo-orbits are used to calculate the Lower Bound Error (LBE). The LLE is the slope of the line gotten from the logarithm of the LBE, which is estimated by means of a recursive least square algorithm (RLS). The main contribution of this paper is to develop a procedure to compute the LLE based on the LBE without using the NIE. Additionally, with the aid of RLS the number of required points has been decreased. Eight numerical examples are given to show the effectiveness of the proposed technique.



## 1. Introduction

It is generally accepted that the largest positive Lyapunov exponent (LLE) is one of the best approaches to detect the presence of chaos in a dynamical system [1–7]. Lyapunov exponents measure the average divergence or convergence of nearby trajectories along certain directions in state space. In chaotic systems, the states of two copies of the same system separate exponentially with time despite very similar initial conditions [8,9]. Several numerical methods to estimate LLE have been proposed since the work by Oseledec [10]. In general, Lyapunov exponents are computed by tracing the exponential divergence of close trajectories. This divergence is explored in [11] to calculate the LLE, although in [12] it is pointed out that such a method is not very robust and difficult to apply. To overwhelm this problem, Rosenstein et al. [1] and Kantz [12] have proposed a different strategy, in which the time dependence of distances between nearby trajectories is recorded explicitly to select the appropriate length scale and range of times from the output [2]. Examples to compute the LLE can be seen in [1,3,6,7,11–14,14–25], just to cite a few.

The relevance of the measure of the LLE and the observation of that two copies of the same system separate exponentially does not rely only on the characterization of the system is chaotic or not. Perc and Marhl [26] have developed a technique in which this featured is exploited to detect and control unstable periodic orbits. It is also important to state that the determination of LLE has been applied with success to acquire important insights into system dynamics [23–25,27]. Recently, Mendes and Nepomuceno [2] have presented a simple algorithm to estimate the LLE. The approach is based on the concept of the lower bound error (LBE) first introduced in [28] and further developed in [29]. To estimate the LLE, the system, either discrete or continuous, is simulated using two different natural interval extensions (NIE), which are the foundation used to calculate the LBE. Although, the method proposed in [2] brings some interesting developments, either for its simplicity and robustness or for the smaller amount of required data, it presents at least one downside, which is the need to elaborate NIE [30]. In a first instance, this seems to be an easy step, but soon we have realised that there are many cases in which NIE are not easily derived. For example, let the quadratic map [31] given by

$$x_{n+1} = 2 - x_n^2. \quad (1)$$

This map is in a very simplified form, which does not allow any change of sequence in the arithmetic operation to produce a different NIE. Besides that, there are dynamical systems, modelled by neural networks, such as in [32], which equations are not easily manipulated. We may also mention systems modelled by blocks, such as Simulink [33], which equations are not explicitly available. Thus, to overcome this limitation, we have found that two differ-

* Corresponding author.
*E-mail addresses:* marciapeixoto93@hotmail.com (M.L.C. Peixoto), nepomuceno@ufsj.edu.br (E.G. Nepomuceno), martins@ufsj.edu.br (S.A.M. Martins), lacerda@ufsj.edu.br (M.J. Lacerda).

https://doi.org/10.1016/j.chaos.2018.04.032
0960-0779/

ent rounding modes present similar effects to those produced by two NIE. Therefore, rounding mode has been applied instead of using NIE to calculate the LBE, and consequently the LLE. According to IEEE 754-2008 standard, the rounding mode indicates how the least significant returned digit of a rounded result is to be calculated [34–36], this can be simply obtained with an internal Matlab function [37] or in C$^{++}$ [38]. From this point, this paper follows the steps presented in [2], where the LLE is obtained by a simple least square fit to the line of the natural logarithm of LBE, just about from the beginning of simulation up to the instant when the LBE stops increasing. We have also improved this stage replacing the least square by the recursive least square algorithm (RLS) [39]. This brings two main advantages: reduction of the number of points and automation of the process, as we do not need to set up beginning and end points of LBE range to calculate the slope, and thus the LLE. As in [1] the natural logarithm is adopted here. The method is applied successfully to eight numerical examples. Firstly, the same examples used in [1]: Logistic [40], Hénon [41], Lorenz [42], and Rössler equations [43] have been considered. We also included other four cases, namely: Sine Map [44], Tent Map [45], Mackey-Glass [46], and a Simulink version of Rössler adapted from Aseeri [47]. We have also investigated the results of the proposed method to calculate the LLE for a periodic dynamical system, which has obviously delivered a non-positive value.

**Algorithm 1** Pseudo-code of the LLE calculation using Matlab, where `mod1` and `mod2` are two different rounding modes and RLS is the recursive least square algorithm according Eq. (6).

**input** Parameters, initial conditions, tol
Stop ← False
**while** Stop **do**
  |system_dependent('setround',mod1)|
  $\hat{x}_{a,n+1} \leftarrow f(\hat{x}_{a,n})$
  |system_dependent('setround',mod2)|
  $\hat{x}_{b,n+1} \leftarrow f(\hat{x}_{b,n})$
  |system_dependent('setround',0.5)|
  $\ell_{\Omega,n+1} \leftarrow (|\hat{x}_{a,n+1} - \hat{x}_{b,n+1}|)/2$
  $\lambda_{n+1} \leftarrow \mathrm{RLS}(\ell_{\Omega,n+1})$
  $\lambda_{5+} \leftarrow \max\{\lambda_{n+1}, \lambda_n, \cdots, \lambda_{n-3}\}$
  $\lambda_{5-} \leftarrow \min\{\lambda_{n+1}, \lambda_n, \cdots, \lambda_{n-3}\}$
  $\lambda_m \leftarrow \mathrm{mean}\{\lambda_{n+1}, \lambda_n, \cdots, \lambda_{n-3}\}$
  **if** $\frac{|\lambda_{5+} - \lambda_{5-}|}{|\lambda_m|} < tol$ **then**
    Stop ← True
  **end if**
**end while**

The remainder of the paper is organised as follows. Section 2 provides preliminary concepts about LBE. The main results are developed in Section 3. Section 4 is devoted to illustrate the results and final remarks are given in Section 5.

## 2. The lower bound error

In this section, some definitions on recursive functions, NIE and pseudo-orbits are shown. After that, the theorem of LBE is presented [28]. Let $n \in \mathbb{N}$, a metric space $M \subset \mathbb{R}$, the relation

$$x_{n+1} = f(x_n), \tag{2}$$

where $f$: $M \to M$, is a recursive function or a map of a state space into itself and $x_n$ denotes the state at the discrete time $n$. The sequence $\{x_n\}$ obtained by iterating Eq. (2) starting from an initial condition $x_0$ is called the orbit of $x_0$ [48]. Let $f$ be a function of real variable $x$. Moore and Moore [49] present the following definition.

**Table 1**
Chaotic systems investigated in this paper. The Rössler has also been modelled using Simulink, as described in Fig. 1. The sampling time is denoted by $\Delta t(s)$. The initial condition is arbitrarily adopted but fixed for the two rounding modes.

| System | Equations | Parameters | $\Delta t(s)$ | Initial Condition |
|---|---|---|---|---|
| Logistic | $x_{n+1} = \mu x_n(1 - x_n)$ | $\mu = 4.0$ | 1 | $x_0 = 2/3$ |
| Hénon | $x_{n+1} = 1 - ax_n^2 + y_n$ | $a = 1.4$ | 1 | $x_0 = 0.3$ |
| | $y_{n+1} = bx_n$ | $b = 0.3$ | | $y_0 = 0.3$ |
| Sine Map | $x_{n+1} = ax_n - bx_n^3$ | $a = 2.6868$ | 1 | $x_0 = 0.1$ |
| | | $b = 0.2462$ | | |
| Tent Map | $x_{n+1} = r\min\{x_n, 1\text{-}x_n\}$ | r=1.99 | 1 | $x_0 = 0.6$ |
| Lorenz | $\dot{x} = \sigma(y - x)$ | $\sigma = 16.0$ | 0.01 | $x(0) = 1$ |
| | $\dot{y} = x(\rho - z) - y$ | $\rho = 45.92$ | | $y(0) = 0.5$ |
| | $\dot{z} = xy - \beta z$ | $\beta = 4.0$ | | $z(0) = 0.9$ |
| Rössler | $\dot{x} = -y - z$ | $a = 0.15$ | 0.10 | $x(0) = -1$ |
| | $\dot{y} = x + ay$ | $b = 0.20$ | | $y(0) = 1$ |
| | $\dot{z} = b + z(x - c)$ | $c = 10.0$ | | $z(0) = 1$ |
| Mackey-Glass | $\dot{x} = \frac{ax_\tau}{1 - x_\tau^c} - bx$ | $a = 0.2,\ b = 0.1$ | 0.3 | $x(0) = 0.3$ |
| | | $c = 10,\ \tau = 30$ | | |

**Table 2**
Computation of the LLE ($\lambda$) given in natural logarithm. The last column presents the number needed iterates to calculate $\lambda$. The expected values are obtained in references indicated in the third column.

| System | Literature $\lambda$ | [Ref.] | Calculated $\lambda$ | Iterates |
|---|---|---|---|---|
| Logistic | 0.693 | [4] | 0.711 | 35 |
| Hénon | 0.418 | [11] | 0.408 | 89 |
| Sine Map | 0.773 | [44] | 0.794 | 26 |
| Tent Map | 0.688 | [45] | 0.684 | 16 |
| Lorenz | 1.500 | [11] | 1.390 | 2496 |
| Rössler | 0.092 | [11] | 0.092 | 1413 |
| Rössler (Simulink) | 0.092 | [11] | 0.092 | 1090 |
| Mackey-Glass | 0.0074 | [18] | 0.0069 | 10,178 |

**Definition 2.1.** A *natural interval extension* (NIE) of $f$ is an interval valued function $F$ of an interval variable $X$, with the property

$$F(x) = f(x) \quad \text{for real arguments}, \tag{3}$$

where by an interval we mean a closed set of real numbers $x \in \mathbb{R}$ such that $X = [\underline{X}, \bar{X}] = \{x : \underline{X} \le x \le \bar{X}\}$.

Connected to a map an orbit may be defined as follows:

**Definition 2.2.** An orbit is a sequence of values of a map, represented by $\{x_n\} = [x_0, x_1, \ldots, x_n]$.

**Definition 2.3.** Let $i \in \mathbb{N}$ represents a *pseudo-orbit, which is defined by an initial condition, a natural interval extension of f, some specific hardware, software, numerical precision standard and discretization scheme*. A pseudo-orbit approximates an orbit and can be represented as

$$\{\hat{x}_{i,n}\} = [\hat{x}_{i,0}, \hat{x}_{i,1}, \ldots, \hat{x}_{i,n}],$$

such that

$$|x_n - \hat{x}_{i,n}| \le \gamma_{i,n}, \tag{4}$$

where $\gamma_{i,n} \in \mathbb{R}$ is a bound of the error and $\gamma_{i,\,n} \ge 0$.

Nepomuceno et al. [29] have shown that two pseudo-orbits derived from associative multiplication property presents the same error bounds. These extensions have been called in such work as *arithmetic interval extension*. The lower bound error theorem has been proved in [29]:

**Theorem 2.4.** *Let $\{\hat{x}_{a,n}\}$ and $\{\hat{x}_{b,n}\}$ be two pseudo-orbits derived from two arithmetic interval extensions. Let $\ell_{\Omega,n} = |\hat{x}_{a,n} - \hat{x}_{b,n}|/2$ be the lower bound error associated to the set of pseudo-orbits $\Omega = [\{\hat{x}_{a,n}\}, \{\hat{x}_{b,n}\}]$ of a map, then $\gamma_{a,n} = \gamma_{b,n} \ge \ell_{\Omega,n}$.*

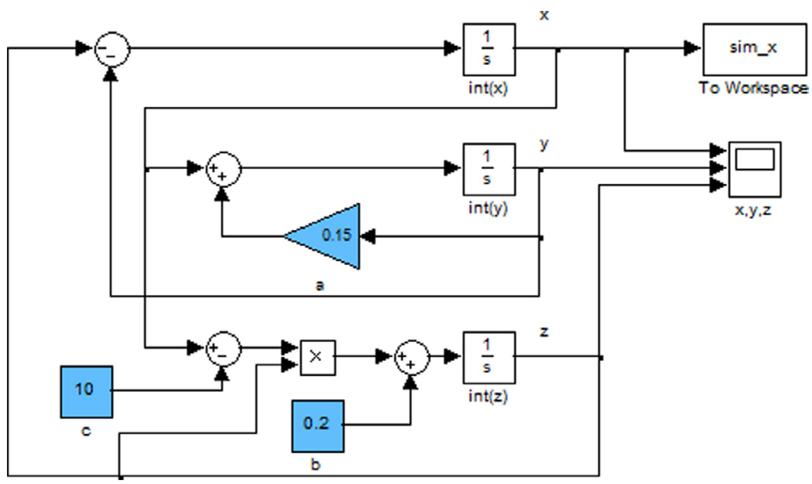


**Fig. 1.** Rössler simulated in Simulink. The parameters, initial condition, sampling time are the same that described in Table 1. Adapted from Aseeri [47].

**Table 3**
Computation of LLE considering two additional combination of rounding modes, namely, rounding upwards ($+\infty$) and rounding to nearest (0.5), and rounding downwards ($-\infty$) and rounding to nearest (0.5).

| System | $+\infty$ and 0.5 | | 0.5 and $-\infty$ | |
|---|---|---|---|---|
| | N | $\lambda$ | N | $\lambda$ |
| Logistic | 35 | 0.709 | 35 | 0.708 |
| Hénon | 89 | 0.408 | 85 | 0.401 |
| Sine Map | 26 | 0.796 | 26 | 0.788 |
| Tent Map | 17 | 0.682 | 12 | 0.685 |
| Lorenz | 2493 | 1.391 | 2529 | 1.396 |
| Rössler | 2436 | 0.087 | 1628 | 0.091 |
| Rössler (Simulink) | 1878 | 0.092 | 2121 | 0.093 |
| Mackey-Glass | 14073 | 0.0074 | 10167 | 0.0069 |

**Table 4**
Critical time $T_c$ using the LLE. See [65] for detailed discussion. $D$ is the diameter of the attractor (the peak-to-peak value). $T_c$ is given in number of iterates for the Logistic, Hénon, Sine Map and Tent Map, and in time for Lorenz, Rössler, Rössler (Simulink) and Mackey-Glass.

| System | $D$ | $LLE_{10}$ | $T_c$ |
|---|---|---|---|
| Logistic | 1 | 0.309 | 51 |
| Hénon | 1 | 0.177 | 89 |
| Sine Map | 1 | 0.345 | 46 |
| Tent Map | 1 | 0.297 | 53 |
| Lorenz | 42.34 | 0.607 | 28.5 |
| Rössler | 17.98 | 0.039 | 425.8 |
| Rössler (Simulink) | 31.89 | 0.039 | 432.6 |
| Mackey-Glass | 1.38 | 0.0030 | 5290.9 |

## 3. Estimating LLE with rounding mode

Normally, the result of an operation (or function) on floating-point numbers cannot be exactly representable in the floating-point system being used, and thus, it must be rounded. One of the most interesting ideas brought out by IEEE 754 is the concept of rounding mode: the way a numerical value is rounded to a finite floating-point number is specified by a rounding mode (or rounding direction attribute), that defines a rounding function [34–36,50]. Denote the set of IEEE 754 floating point numbers (including gradual underflow and $\pm\infty$) by $\mathbb{F}$, includes directed rounding. We can use different rounding modes, such as: $\square$ rounding to nearest, $\triangledown$ rounding downwards (towards $-\infty$), and $\triangle$ rounding upwards (towards $+\infty$). For example, let $a, b, c \in \mathbb{F}$. Then,

$$d_1 = \triangledown(a \times b - c)$$
$$d_2 = \triangle(a \times b - c)$$

produces $d_1, d_2 \in \mathbb{F}$ such that the true result $d = a \times b - c \in \mathbb{R}$ satisfies $d_1 \leq d \leq d_2$. Note that this does not need be true when replacing $a \times b - c$ by $c - a \times b$. Switching rounding mode is available in Matlab through an internal routine: `system_dependent('setround',mod)`, where `mod=-Inf` or `mod=Inf` switches the rounding mode to downwards or upwards, respectively. For `mod=0.5` the rounding mode is set to the nearest [37]. This procedure may also be achieved in other programming languages, such as in C++ [38]. In this case, the pseudo-orbits $\{\hat{x}_{a,n}\}$ and $\{\hat{x}_{b,n}\}$ are derived from two rounding modes, instead of two NIE, as proposed by Mendes and Nepomuceno [2]. It is important to stress that we are using only rounding modes defined by IEEE 754-2008.

The method proposed in this work is summarised in the following steps:

1. Choose two rounding modes. In this paper, we show the results for all possible permutations of the three basic rounding modes: rounding to nearest, rounding downwards and rounding upwards;
2. With the same software, hardware, operational system, initial conditions, step size and discretization scheme, simulate the system with two previously chosen rounding modes;
3. Use the recursive least square algorithm (RLS) to estimate the slope of absolute value of natural algorithm of the LBE. The slope of this line is the LLE.

The implementation of the proposed method can be easily made, merely inserting the suitable functions in the routine. Regarding the third step, the slope is estimated by means of RLS. Let a model be represented such as [39,51]:

$$y(k) = \psi_k^T(k-1)\hat{\theta}_{\mathbf{k}} + \xi(k), \tag{5}$$

where a sequence of computed LBE are presented in $\psi^T(k-1)$ and $y(k)$; $\xi(k)$ is the residue at time $k$ and $\hat{\theta}_k$ are the parameters to be estimated, which are the slope (LLE) and independent term for the line. The parameter $\hat{\theta}_k$ are estimated by means of the following equations:

$$\begin{cases} K_k = \frac{P_{k-1}\psi_k}{\psi_k^T P_{k-1}\psi_k + 1}, \\ \hat{\theta}_k = \hat{\theta}_{k-1} + K_k\Big[y(k) - \psi_k^T\hat{\theta}_{k-1}\Big], \\ P_k = P_{k-1} - K_k\psi_k^T P_{k-1}, \end{cases} \tag{6}$$

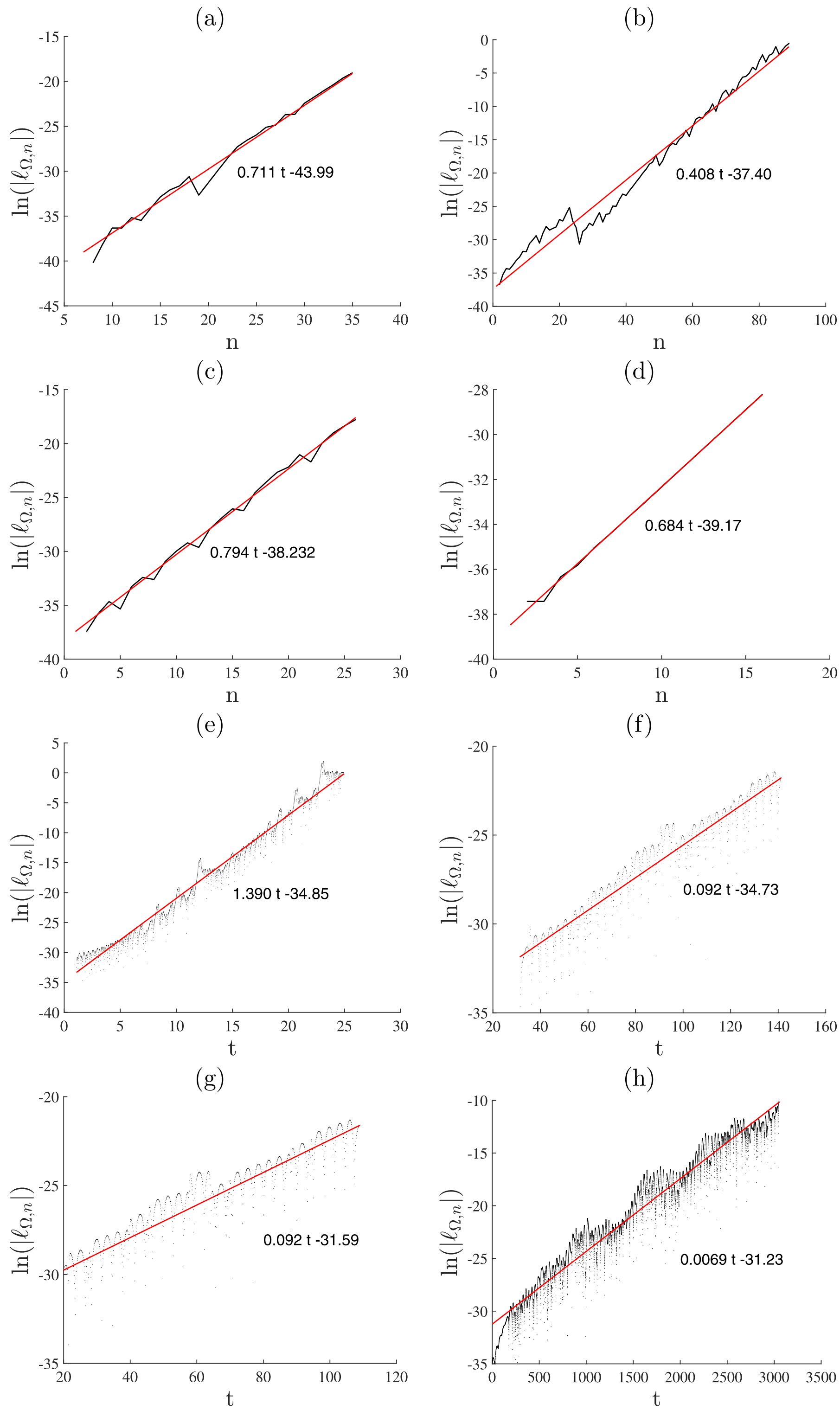


**Fig. 2.** The LBE for the chaotic dynamical systems, where (a) Logistic, (b) Hénon, (c) Sine Map, (d) Tent Map, (e) Lorenz, (f) Rössler, (g) Rössler (Simulink) and (h) Mackey-Glass. The red line is the least squares fit. In each figure, the equation of the line is also shown, where the first value is the estimate of the LLE. The x-axis is time and y-axis is $\ln(|\ell_{\Omega,n}|)$. The calculation of $\ell_{\Omega,n}$ is performed as described in Theorem 2.4. (For interpretation of the references to color in this figure legend, the reader is referred to the web version of this article.)

where $K_k$ is the gain matrix, $P_k$ is the covariance matrix, $\psi$ is the regressors matrix at time $k$, and $y(k)$ is the vector of dependent variable. The initial conditions adopted are: $P_0 = 10^4 \mathrm{I}_2$ and $\theta_{\mathbf{0}} = [0 \quad 0]^{\mathrm{T}}$. A pseudo-code of the LLE calculation using Matlab is presented in Algorithm 1.

As presented in [28,29], the LBE is a measure of the distance between the simulated dynamical systems (or pseudo-orbit) and the real orbit. If a system is chaotic the distance between these two entities must be exponentially divergent, and therefore a slope in a logarithm plot of the LBE is what is needed to capture such a divergence and quantified it as a number which is precisely the

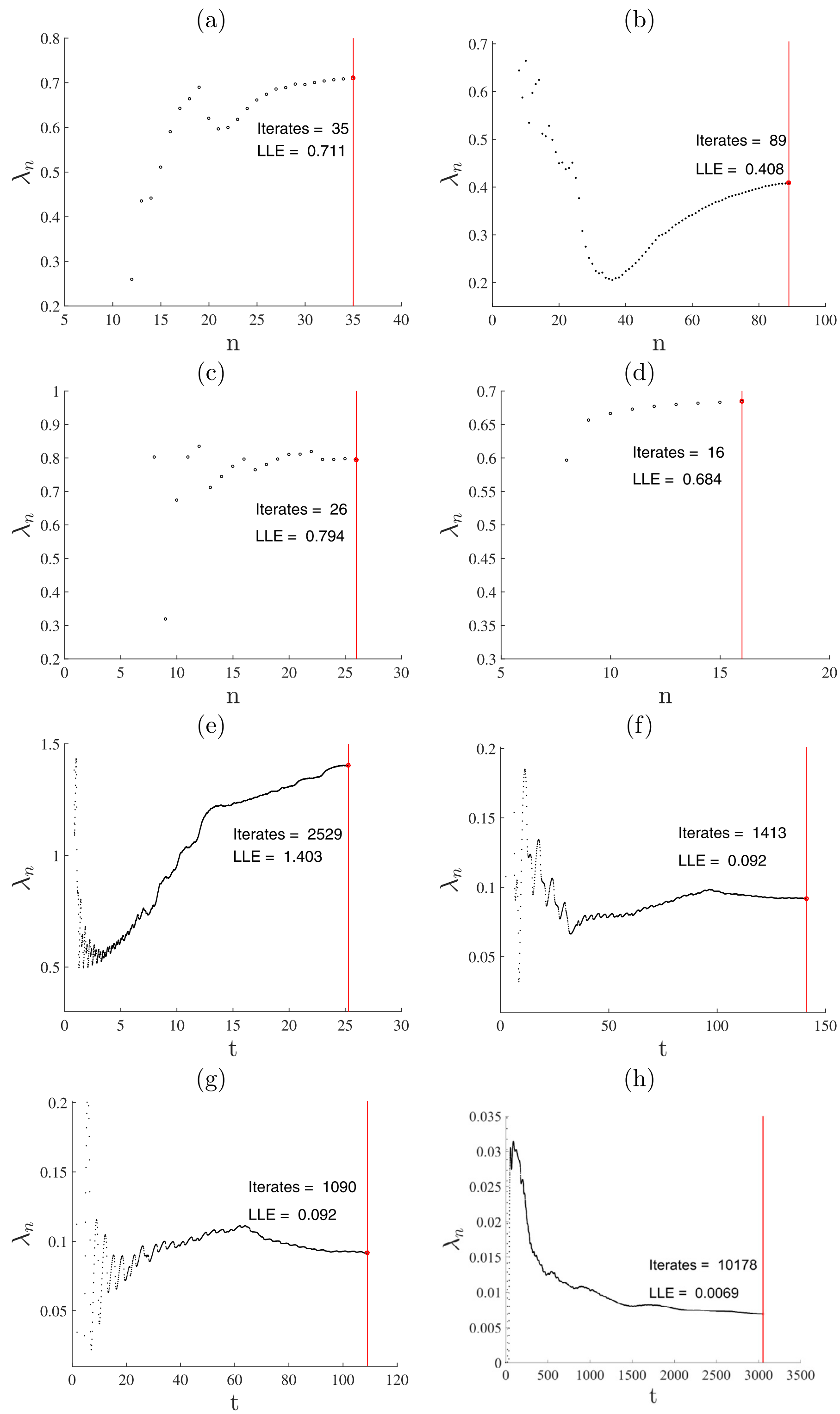


**Fig. 3.** The convergence to LLE of the numerical examples, where (a) Logistic, (b) Hénon, (c) Sine Map, (d) Tent Map, (e) Lorenz, (f) Rössler, (g) Rössler (Simulink) and (h) Mackey-Glass. The red line indicates where the stop criteria has been reached. X-axis is time and y-axis is the LLE. In each graph, it is also shown the number of required iterates and the computed LLE. We have established the tolerance for the examples (a), (c), (d) as $tol = 0.01$, for example (b) as $tol = 0.005$, for example (e) as $tol = 0.00003$, for examples (f) and (g) as $tol = 0.00005$ and for example (h) as $tol = 0.000001$. (For interpretation of the references to color in this figure legend, the reader is referred to the web version of this article.)

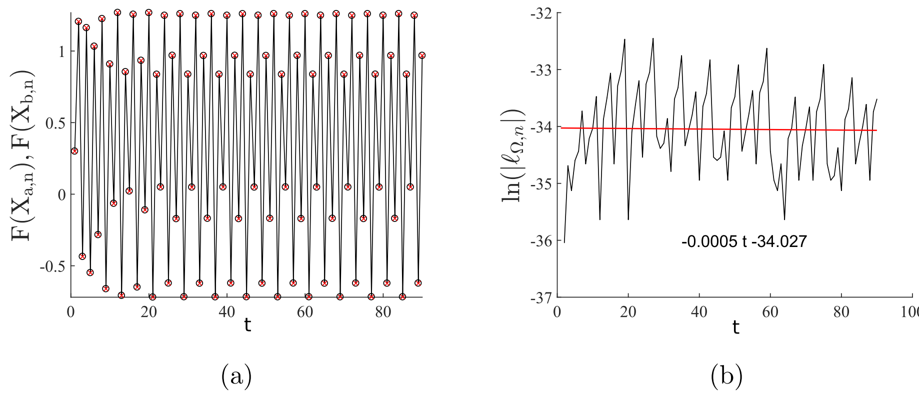


**Fig. 4.** Hénon map: (a) Results of $n$ iterates for two pseudo-orbits, which have been yield by means of rounding downwards (o) and rounding upwards (x). (b) The LBE for the Hénon Map, wherein the calculation of $\ell_{\Omega,\, n}$ is performed as described in the Theorem 2.4.

definition of the positive Lyapunov exponent. Thus, the definition of the largest Lyapunov exponent used by Rosenstein et al. [1] is considered

$$d(t) = Ce^{\lambda t}, \tag{7}$$

where $d(t)$ is the average divergence at time $t$, $C$ is a constant that normalises the initial separation and the $\lambda$ is the Lyapunov exponent (LLE). Using (7) combined with LBE definition and chaotic system, one can easily understand why it is possible to estimate the LLE using the proposed method.

## 4. Illustrative examples

In this section, the proposed method is applied to calculate the largest positive Lyapunov exponent from the chaotic systems described in Table 1. To show some properties of the proposed method, one of the chaotic system, the Rössler has also been modelled using Simulink from an adaptation of a work done by Aseeri [47], as shown in Fig. 1. All simulations were performed using Matlab in a computer with double precision (64 bits). The continuous systems were discretised using the fourth order Runge-Kutta method. In the end of section, we have also shown the ability of the method to distinguish non chaotic orbits.

Table 2 shows the results obtained in calculating the LLE. The natural logarithm of LBE and the fitted line are shown in Fig. 2 with their respective equation. The estimated LLE is in good agreement with the values found in the literature. Besides, the number of iterations is also presented and they are much smaller than those values presented for the maps in [1]. It is noteworthy that to implement the presented approach one does not need any kind of parametrization or embedding dimension. The method makes use only of the simulation of two rounding modes of the original dynamic equation, making the computation of the LLE quite simple. Comparing with the previous work of the authors [2], the reduction of the number of iterates is significant. The number of iterates has dropped in all the five systems tested, with a minimum of decrease of 15% for the Lorenz and reaching 60% for the Rössler. Other important features of the proposed method are outlined here. First, the method has been tested with a great variety of systems. From discrete to continuous systems, as well as high order systems, such as Mackey-Glass system. Compared to previous work [2] two systems have been tested in order to show the superiority of the proposed method. The first system is the Tent Map. Although this system is simple, it presents the same problem described in (1), as it does not allow the derivation of NIE. Even if NIE are easily derived from systems such as Lorenz and Logistic Map, this procedure relies on a symbolic manipulation, which for the sake of algorithm automation is not usually straightforward. The second system is the Rössler simulated by Simulink (see Fig. 1). In both cases, the pseudo-orbit is easily produced without any problem. We have also presented an example to deal with computation of LLE from data, which is an important feature for model-free investigations. The example of the Sine Map shows the possibility to combine the proposed method and system identification tools. In fact, the Sine Map, described in [44], is given by

$$x_{n+1} = 1.2\pi \sin(x_n), \tag{8}$$

whereas the Sine Map used to estimate the LLE has been given by

$$x_{n+1} = 2.6868x_n - 0.2462x_n^3, \tag{9}$$

as indicated in Table 1. Instead of using the original equation, we deliberately apply a polynomial NAR identified from the data. The literature is full of examples of system identification approach to model chaotic systems, [52] which allows the proposed method to be applied even in cases where there are no known equations of the system. The interesting reader may consult [53] for further details on this topic.

For the systems introduced in the Table 1, we have also tested more two combinations of rounding modes, in order to verify the robustness of the proposed method. Table 3 provides the results, which show good agreement with the literature. The connection between chaos and finite precision also deserves a remark here. Works such as in [28,54–64] have been extensively investigated the effects of finite precision in the simulation of chaotic systems in many perspectives and in many sorts of systems. Using the LLE as a sort of propagation error measurement, we also estimate the maximum number of iterations wherein the simulation relies on a required precision or number of significant digits. To carry out this analysis we use Eq. (10), detailed in [65]:

$$T_c = \frac{\log_{10}(D/2) + P}{LLE_{10}}, \tag{10}$$

where $T_c$ is the maximum number of iterations (or time), $D$ is the diameter of the attractor, or its peak-to-peak value, $P$ is the number of significant digits (for 64bits, $P \approx 16$), and $LLE_{10}$ is given in the logarithm to base ten. The LLE (calculated) given in Table 2 is easily changed into base ten by means of

$$LLE_{10} = \log_{10}(e^{LLE}).$$

Table 4 shows an estimation of the maximum number of iterations or time ($T_c$). For $t > T_c$, the simulation is no longer reliable, and all the significant digits are lost. In such situation, it is highly advisable to carry out a more detailed investigation before to make any conclusion. (Fig. 3)

Finally, we have tested the method for the case of non-chaotic orbits. Considering the Hénon Map with parameters: $a = 1.05,\ b =$

0.3 and initial conditions $x_0 = 0.3$ and $y_0 = 0.3$. Two pseudo-orbits have been yield by means of rounding downwards (towards $-\infty$) and rounding upwards (towards $+\infty$). As can be seen in Fig. 4 (a) the map is in a periodicity region. Thereby, when we compute the LBE there is no exponentially divergence and the inclination of the fitted line is approximately zero, as shown in Fig. 4 (b).

## 5. Conclusions

Prior work has documented the effectiveness of using the lower bound error (LBE) to compute the largest positive Lyapunov exponent (LLE) [2]. However, these studies require the elaboration of natural interval extensions, which are not generally easy to obtain or even feasible to be developed. In this paper, we have introduced a method to calculate the LLE using two rounding modes of the same equation. The method proposed does not need any sort of parametrization, embedding dimension, estimation of the linearized and natural interval extension of the original dynamic equation, only the use of two rounding modes and the original dynamic equation and recursive least square algorithm. The use of rounding mode is a procedure that does not make use of symbolic manipulations, and it can be used in systems such as the Rössler modelled in Simulink (Fig. 1) or in models which the NIE is not possible to be derived. We have also tested successfully the method with an identified model from data (Sine Map). Instead of using its original equation, we have applied an identified polynomial NAR. The results are in good agreement, showing that the combination of the proposed approach and system identification tools, such as polynomial NARMAX [52], allows the computation of the LLE from time series, as it has successfully been accomplished in [53]. The estimates of the LLE using the proposed method were shown to be in a good agreement with the values found in the literature when considering well-known chaotic systems. Moreover, the proposed method can be considered as a simple tool to search for new chaotic systems, because the computational of long and demanding calculations to estimate the LLE is no longer needed. It has also been shown the effectiveness of the method to identify non-chaotic systems, as seen in Fig. 4. In fact, with the aid of the RLS we could reduce the number of points used by Mendes and Nepomuceno [2]. The use of rounding mode and RLS have also presented the benefits of the automation of the routine, which in [2] it is required a symbolic manipulation of the model, normally performed by the user.

Apart from that, we believe that this characterisation of chaotic systems suggests a connection between chaos and the finite precision of computer arithmetic, as the LLE may also be used to indicate the range time limit, in which the simulation is within a required precision or a specific number of significant digits. This is certainly an issue which deserves more investigation to shed light in many issues on nonlinear dynamics highly dependent from numerical simulations. Like the results obtained in [2], this paper shows that the Lyapunov exponent is close related to the propagation error of a computer simulation in a finite precision machine. In fact, the technique reported in this paper is nothing less than a measure of the error due to finite precision, which quite surprisingly, it is exactly the LLE.

## Acknowledgements

This work has been supported by CNPq/INERGE, FAPEMIG and CAPES.

## References

[1] Rosenstein MT, Collins JJ, De Luca CJ. A practical method for calculating largest Lyapunov exponents from small data sets. Physica D 1993;65(1–2):117–34.
[2] Mendes EMAM, Nepomuceno EG. A very simple method to calculate the (positive) largest lyapunov exponent using interval extensions. Int J Bifurcation Chaos 2016;26(13):1650226.
[3] Dabrowski A. Estimation of the largest Lyapunov exponent from the perturbation vector and its derivative dot product. Nonlinear Dyn 2012;67(1):283–291.
[4] Eckmann JP, Ruelle D. Ergodic theory of chaos and strange attractors. Rev Mod Phys 1985;57(3):617–56.
[5] Li C, Chen G. Estimating the Lyapunov exponents of discrete systems. Chaos 2004;14(2):343–6.
[6] Yao T-L, Liu H-F, Xu J-L, Li W-F. Estimating the largest Lyapunov exponent and noise level from chaotic time series. Chaos 2012;22(3):033102.
[7] Matsuoka C, Hiraide K. Computation of entropy and Lyapunov exponent by a shift transform. Chaos 2015;25(10):103110.
[8] Odavić J, Mali P, Tekić J, Pantić M, Pavkov-Hrvojević M. Application of largest Lyapunov exponent analysis on the studies of dynamics under external forces. Commun Nonlinear Sci Numer Simul 2017;47:100–8.
[9] Nazarimehr F, Jafari S, Hashemi Golpayegani SMR, Sprott JC. Can Lyapunov exponent predict critical transitions in biological systems? Nonlinear Dyn 2017;88(2):1493–500.
[10] Oseledec VI. The multiplicative ergodic theorem: the Lyapunov characteristic numbers of dynamical systems. Trans Moscow Math Soc 1968;19:197–231.
[11] Wolf A, Swift JB, Swinney HL, Vastano JA. Determining Lyapunov exponents from a time series. Physica D 1985;16(3):285–317.
[12] Kantz H. A robust method to estimate the maximal Lyapunov exponent of a time series. Phys Lett A 1994;185(1):77–87.
[13] Franchi M, Ricci L. Statistical properties of the maximum Lyapunov exponent calculated via the divergence rate method. Phys Rev E 2014;90(6):062920.
[14] Kim BJ, Choe GH. High precision numerical estimation of the largest Lyapunov exponent. Commun Nonlinear Sci Numer Simul 2010;15(5):1378–84.
[15] He J, Yu S, Cai J. Numerical analysis and improved algorithms for Lyapunov–exponent calculation of discrete-time chaotic systems. Int J Bifurcation Chaos 2016;26(13):1650219.
[16] Benettin G, Galgani L, Giorgilli A, Strelcyn J-M. Lyapunov characteristic exponents for smooth dynamical systems and for Hamiltonian systems; a method for computing all of them. part 1: theory. Meccanica 1980;15(1):9–20.
[17] Gavilán-Moreno CJ, Espinosa-Paredes G. Using largest Lyapunov exponent to confirm the intrinsic stability of boiling water reactors. Nucl Eng Technol 2016;48(2):434–47.
[18] Sano M, Sawada Y. Measurement of the Lyapunov spectrum from a chaotic time series. Phys Rev Lett 1985;55(10):1082–5.
[19] Brown R, Bryant P, Abarbanel HDI. Computing the Lyapunov spectrum of a dynamical system from an observed time series. Phys Rev A 1991;43(6):2787–806.
[20] Rangarajan G, Habib S, Ryne RD. Lyapunov exponents without rescaling and reorthogonalization. Phys Rev Lett 1998;80(17):3747–50.
[21] Geist K, Parlitz U, Lauterborn W. Comparison of different methods for computing Lyapunov exponents. Prog Theor Phys 1990;83(5):875–93.
[22] Souza SLT, Caldas IL. Calculation of lyapunov exponents in systems with impacts. Chaos, Solitons Fractals 2004;19(3):569–79.
[23] Kodba S, Perc M, Marhl M. Detecting chaos from a time series. Eur J Phys 2005;26(1):205–15.
[24] Perc M. Nonlinear time series analysis of the human electrocardiogram. Eur J Phys 2005;26(5):757–68.
[25] Perc M. The dynamics of human gait. Eur J Phys 2005;26(3):525–34.
[26] Perc M, Marhl M. Detecting and controlling unstable periodic orbits that are not part of a chaotic attractor. Phys Rev E 2004;70(1):016204.
[27] Zadeh HG, Haddadnia J, Montazeri A. A model for diagnosing breast cancerous tissue from thermal images using active contour and Lyapunov exponent. Iran J Public Health 2016;45(5):657.
[28] Nepomuceno EG, Martins SAM. A lower bound error for free-run simulation of the polynomial NARMAX. Syst Sci Contr Eng 2016;4(1):50–8.
[29] Nepomuceno EG, Martins SAM, Amaral GFV, Riveret R. On the lower bound error for discrete maps using associative property. Syst Sci Contr Eng 2017. Accepted.
[30] Moore RE, Kearfott RB, Cloud MJ. Introduction to interval analysis. SIAM; 2009. ISBN 9780898716696.
[31] Ramadan N, Ahmed HEH, Elkhamy SE, El-samie FEA. Chaos-based image encryption using an improved quadratic chaotic map. Am J Sign Proc 2016;6(1):1–13.
[32] Nepomuceno EG. Multiobjective learning in the random neural network. Int J Adv Intell Paradigms 2014;6(1):66.
[33] Nepomuceno EG, Takahashi RHC, Aguirre La, Neto OM, Mendes EMAM. Multiobjective nonlinear system identification: a case study with thyristor controlled series capacitor (TCSC). Int J Syst Sci 2004;35(9):537–46.
[34] Goldberg D. What every computer scientist should know about floating-point arithmetic. Comput Surv 1991;23(1):5–48.
[35] Institute of Electrical and Electronics Engineers (IEEE). IEEE standard for floating-Point arithmetic. IEEE Std 754-20082008;:1–70.
[36] Overton ML. Numerical computing with IEEE floating point arithmetic. Society for Industrial and Applied Mathematics; 2001.
[37] Rump SM. High precision evaluation of nonlinear functions. In: Proceedings of 2005 international symposium on nonlinear theory and its applications, Bruge, Belgium, October 18, 21; 2005. p. 733–6.
[38] Fukasawa R, Poirrier L. Numerically safe lower bounds for the capacitated vehicle routing problem. INFORMS J Comput 2017;29(3):544–57.

[39] Oliveira P, Seixas P, Aguirre L, Peixoto Z. Parameter estimation of a induction machine using a continuous time model. In: IECON '98. Proceedings of the 24th annual conference of the ieee industrial electronics society (Cat. No.98CH36200), 1. IEEE; 1998. p. 292–6. ISBN 0-7803-4503-7.
[40] May RM. Simple mathematical models with very complicated dynamics.. Nature 1976;261(5560):459–67.
[41] Hénon M. A two-dimensional mapping with a strange attractor. Commun Math Phys 1976;50(1):69–77.
[42] Lorenz EN. Deterministic nonperiodic flow. J Atmos Sci 1963;20:283–93.
[43] Rössler O. An equation for continuous chaos. Phys Lett A 1976;57(5):397–8.
[44] Nepomuceno EG, Takahashi RHC, Amaral GFV, Aguirre LA. Nonlinear identification using prior knowledge of fixed points: a multiobjective approach. Int J Bifurcation Chaos 2003;13(05):1229–46.
[45] Yoshida T, Mori H, Shigematsu H. Analytic study of chaos of the tent map: band structures, power spectra, and critical behaviors. J Stat Phys 1983;31(2):279–308.
[46] Mackey M, Glass L. Oscillation and chaos in physiological control systems. Science 1977;197(4300):287–9.
[47] Aseeri MAS. Chaotic model (Rossler) using filed programmble gate array (FPGA). In: 2009 4th international design and test workshop (IDT). IEEE; 2009. p. 1–4. IDT.2009.5404083. ISBN 978-1-4244-5748-9.
[48] Gilmore R, Lefranc M. The topology of chaos: alice in stretch and squeezeland. John Wiley & Sons; 2012.
[49] Moore RE, Moore RE. Methods and applications of interval analysis, 2. Philadelphia: SIAM; 1979.
[50] Muller J-M, Brisebarre N, De Dinechin F, Jeannerod C-P, Lefevre V, Melquiond G, et al. Handbook of floating-point arithmetic. Springer Science & Business Media; 2009.
[51] Ljung L. System identification: theory for the user.. London: Prentice-Hall; 1987.
[52] Billings SA. Nonlinear system identification: NARMAX methods in the time, frequency, and spatio-temporal domains. West Sussex: John Wiley & Sons; 2013.
[53] Nepomuceno EG, Martins SAM, Lacerda MJ, Mendes EMAM. On the use of interval extensions to estimate the largest Lyapunov exponent from chaotic data. Math Probl Eng 2018;v. 2018:1–8.
[54] Corless RM. What good are numerical simulations of chaotic dynamical systems? Comput Math Appl 1994;28(10):107–21.
[55] Corless RM, Essex C, Nerenberg MAH. Numerical methods can suppress chaos. Phys Lett A 1991;157(1):27–36.
[56] De Markus AS. Detection of the onset of numerical chaotic instabilities by Lyapunov exponents. Discrete Dyn Nat Soc 2001;6(2):121–8.
[57] Galias Z. The dangers of rounding errors for simulations and analysis of nonlinear circuits and systems - and how to avoid them. IEEE Circuits Syst Mag 2013;13(3):35–52.
[58] Leonov GA, Andrievskiy BR, Mokaev RN. Asymptotic behavior of solutions of Lorenz-like systems: analytical results and computer error structures. Vestnik St Petersburg University, Mathematics 2017;50(1):15–23.
[59] Lorenz EN. Computational chaos-a prelude to computational instability. Physica D 1989;35(3):299–317.
[60] Lozi R. Can we trust in numerical computations of chaotic solutions of dynamical systems?. In: Topology and dynamics of chaos: in celebration of Robert Gilmore's 70th Birthday. Edited by Letellier Christophe. Published by World Scientific Publishing Co. Pte. Ltd., 1; 2013. p. 63–98.
[61] Nepomuceno EG. Convergence of recursive functions on computers. J Eng 2014:1–3.
[62] Ni J, Liu L, Liu C, Hu X, Li S. Fast fixed-time nonsingular terminal sliding mode control and its application to chaos suppression in power system. IEEE Trans Circuits Syst II Express Briefs 2017;64(2):151–5.
[63] Varsakelis C, Anagnostidis P. On the susceptibility of numerical methods to computational chaos and superstability. Commun Nonlinear Sci Numer Simul 2016;33:118–32.
[64] Yao L-S. Computed chaos or numerical errors. Nonl Anal 2005;15(1):109–26.
[65] Nepomuceno EG, Mendes EMAM. On the analysis of pseudo-orbits of continuous chaotic nonlinear systems simulated using discretization schemes in a digital computer. Chaos Solitons Fractals 2017;95:21–32.